Journal of Hydrology 394 (2010) 198–212

Contents lists available at ScienceDirect

Journal of Hydrology

journal homepage: www.elsevier.com/locate/jhydrol

Generalised synthesis of space–time variability in flood response: An analytical framework

Alberto Viglione [a,*], Giovanni Battista Chirico [b], Ross Woods [c], Günter Blöschl [a]

[a] Institut für Wasserbau und Ingenieurhydrologie, Technische Universität Wien, Vienna, Austria
[b] Dipartimento di Ingegneria Agraria, Università di Napoli Federico II, Naples, Italy
[c] National Institute for Water and Atmospheric Research (NIWA), Christchurch, New Zealand

ARTICLE INFO

Keywords:
Storm movement
Spatial patterns
Correlation
Runoff generation
Runoff coefficient
Hydrologic theory

SUMMARY

We extend the method developed by Woods and Sivapalan (1999) to provide a more general analytical framework for assessing the dependence of the catchment flood response on the space–time interactions between rainfall, runoff generation and routing mechanisms. The analytical framework focuses on three characteristics of the flood hydrograph: the catchment rainfall excess rate, and the first and second temporal moments of the flood response. These characteristics are described by analytical relations, which are derived with a limited number of assumptions concerning the catchment response that comply well with many modelling approaches. The paper illustrates the development of the analytical framework and explains the conceptual meaning of the mathematical relations by taking a simple and idealised "open-book" catchment as a case study. It is shown how the components of the derived equations explicitly quantify the relative importance of processes and the space–time interactions among them during flood events. In particular, the components added to the original framework of Woods and Sivapalan (1999), which account for storm movement and hillslope routing variability in space, are demonstrated to be important and in some cases decisive in combining to bring about the flood response. The proposed analytical framework is not a predictive model but a tool to understand the magnitude of the components that contribute to runoff response, similar to the components of the St. Venant equations in fluid dynamics.

1. Introduction

Catchment flood response is the result of numerous hydrological processes, characterised by significant levels of spatial and temporal variability. Many hydrological studies have focused on the role of hydrological space–time variability in catchment response, with the aim of developing a rationale for more effective catchment monitoring, modelling and forecasting (e.g., Skøien et al., 2003; Skøien and Blöschl, 2006). From a practical perspective, it is important to know at what space–time scales catchment processes have to be observed, which sources of variability are crucial to understanding catchment response, and what are the effects of space–time aggregations in model simulations. Many of the space–time interactions between processes in catchment response have been studied but rarely in a single comprehensive framework. The need for generalisation is one of the aspects that distinguish catchment hydrology from other disciplines (Blöschl, 2005) and to which the hydrological community is directing its efforts (Sivapalan, 2005). With what has been termed *comparative hydrology*, common methods are sought for assessing and quantifying hydrological similarity, e.g., through comparisons between events in a catchment or between catchments in different hydrologic regimes (McDonnell and Woods, 2004; Blöschl, 2006). In this respect, the formulation of a simple coherent framework, which describes parsimoniously the functioning of catchment response and which focuses on the order of magnitudes of the processes, may assist. Such a framework may give the order of magnitude of process components in much the same way as the terms of the St. Venant equations can be used to provide insight into whether, e.g., diffusive processes are important for flood routing or not. This assessment is conveniently summarised through the use of dimensionless numbers (Wagener et al., 2007).

Woods and Sivapalan (1999) outlined such an analytical framework, which quantifies the effects of flood event space–time variability on catchment storm response using several assumptions concerning the space–time structure of the hydrological patterns and runoff routing. This framework is generally applicable to any simulated or observed data-set and defines the effects of hydrological variability by a few indices of clear physical meaning. A practical method of this type can be employed to identify the measurement or modelling variables to be given priority over less

* Corresponding author. Tel.: +43 1 58801 22317.
E-mail address: viglione@hydrol.tuwien.ac.at (A. Viglione).

0022-1694/$ - see front matter © 2010 Elsevier B.V. All rights reserved.
doi:10.1016/j.jhydrol.2010.05.047

important features. The paper of Woods and Sivapalan (1999) develops and illustrates analytical results in the case where complex space and time variability of both rainfall and runoff generation are included as well as hillslope and channel network routing. It characterizes storm response with three quantities: (i) the storm-averaged value (i.e., storm rainfall excess), (ii) the mean runoff time (i.e., the time of the centre of mass of the runoff hydrograph at a catchment outlet), and (iii) the variance of the timing of runoff (i.e., the temporal dispersion of the runoff hydrograph). The mean time of catchment runoff is a surrogate for the time to peak. The storm-averaged rainfall excess rate and the variance of runoff time, taken together, are indicative of the magnitude of the peak runoff. For a given event duration and volume of runoff, a sharply peaked hydrograph will have a relatively low variance compared to a more gradually varying hydrograph (see Woods (1997) for details).

In this paper we significantly extend the theory proposed by Woods and Sivapalan (1999) by relaxing two of their most restrictive assumptions. The first is the assumption of multiplicative space–time separability for both rainfall and runoff generation processes. Precipitation and runoff coefficient, according to this assumption, are neither constant in time nor uniform in space but their spatial pattern (i.e., the relative spatial distribution of them) does not change in time, and their temporal pattern does not change in space. Crudely speaking, this implies that the storm event is stationary, i.e., it does not move over the catchment. This is quite a strong assumption indeed and, as will be shown, can be relaxed at the cost of introducing some new terms in the analytical expressions. The second assumption of Woods and Sivapalan (1999) is that the distribution of hillslope travel times is spatially uniform, which is also relaxed in the present paper. We account for spatial variability of the hillslope routing time throughout the catchment, but we still assume that it is constant in time. Regarding the channel routing, we retain the constant velocity assumption made by Woods and Sivapalan (1999), which has been shown to be reasonable for flood routing purposes (Pilgrim, 1976; Beven, 1979). This velocity corresponds to the celerity of a flood wave in a stream network. Following Rinaldo et al. (1991), we also assume that geomorphological dispersion (caused by the distribution of travel distances in a channel network) dominates the effects of hydrodynamic dispersion, which we neglect. The remaining assumptions we make here (i.e., hillslope response constant in time and stream velocity constant in time and space) are common to the majority of the models applied for simulating distributed catchment response to storm events and are believed to meet our immediate objective of providing insight into the complex interactions among the key variables affecting flood response.

The catchment flood response is conceptualised into three fundamental stages: (i) rain falls on the catchment and either becomes rainfall excess through the action of a runoff generation process or is stored, (ii) rainfall excess is routed to the base of hillslopes (where it enters the channel) and (iii) hillslope outflow is then routed along channels to the catchment outlet (where it becomes catchment runoff). It is important to note that the framework is not intended to be a predictive model but a tool that can quantify the relative importance of the processes involved in flood response and the space–time interactions between rainfall and catchment state during flood events.

In this paper we derive the equations for the catchment rainfall excess and the catchment runoff time in a similar way as in Woods and Sivapalan (1999). Purely to illustrate the meaning of the terms of the equations, we provide examples of their values for artificially prescribed storm events affecting the stylised stream-catchment system represented in Fig. 1. The stylised catchment is divided into five "open-book" parts, each characterised by a different artificially prescribed temporal evolution of the runoff coefficient and a different hillslope response time. Also, the network response time of each part is 1 time step (e.g., 1 h). Thus the water entering the network in part 5 needs 5 time steps (e.g., 5 h) to reach the outlet while the water entering the network in part 1 needs 1 time step. We consider different spatially-variable storm events of duration 6 time steps, occurring on this stylised catchment. In all cases the catchment average rainfall volume is 100 units (e.g., 100 mm) and the catchment average (in space and time) runoff coefficient is equal to 0.3. Since the overall rainfall volume and runoff coefficient are the same for all events, the differences between catchment responses are caused by the spatio-temporal variability of rainfall and runoff coefficient, the spatial variability of the hillslope routing, the distance to the outlet (channel routing) and the interaction between them. With this simple and idealised case study, in which space is one-dimensional and symmetric to time, we can easily investigate and illustrate the meaning of the analytical terms in the equations derived below. It is important to note that the equations are not derived to describe this simplified system but are general and apply to any catchment configuration.

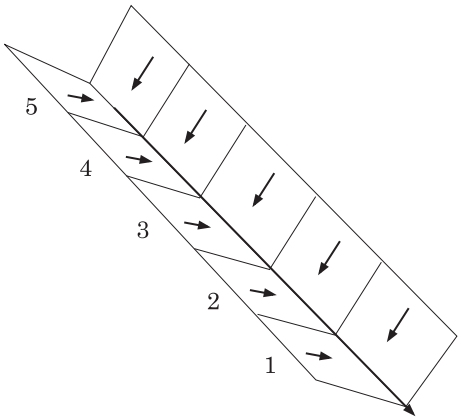

Fig. 1. Stylised open book catchment with a single stream.

2. Catchment rainfall excess

Following Woods and Sivapalan (1999), we define the rainfall excess $R(x,y,t)$ [LT^{-1}] at location (x,y) and at time t as follows:

$$R(x,y,t) = P(x,y,t) \cdot W(x,y,t) \quad (1)$$

where $P(x,y,t)$ [LT^{-1}] is the local rainfall and $W(x,y,t)$ [·] is the local runoff coefficient, bounded between 0 and 1.

Fig. 2 represents four different events, one for each row, occurring in the stylised catchment of Fig. 1. These are spatio-temporal graphs where $D(x,y)$ [L] denotes the distance to the outlet, v [LT^{-1}] the flow velocity in the streams, and t [T] the time, which ranges from 0 to 6. In the first event, referred hereafter as E1, the precipitation is uniform in space but varies in time. It increases rapidly after the beginning of the event and has its maximum at the second time step. The runoff coefficient, instead, varies both in space and in time. It increases in time and has its maximum close to the catchment outlet ($D(x,y)/v$ between 0 and 1). The effective rainfall given by this event is concentrated in the first two time steps, when the rainfall is high, and close to the outlet. In the second event (E2) the rainfall also varies both in time and space. The effective rainfall in this case is more intense and localised than in the first example. The third rainfall event (E3) represents a moving storm which is intense close to the outlet at the beginning of the event and then moves upstream. In this case the runoff coefficient does not vary so much within the catchment (in space), nor in time. The local effective rainfall is much less intense than in the

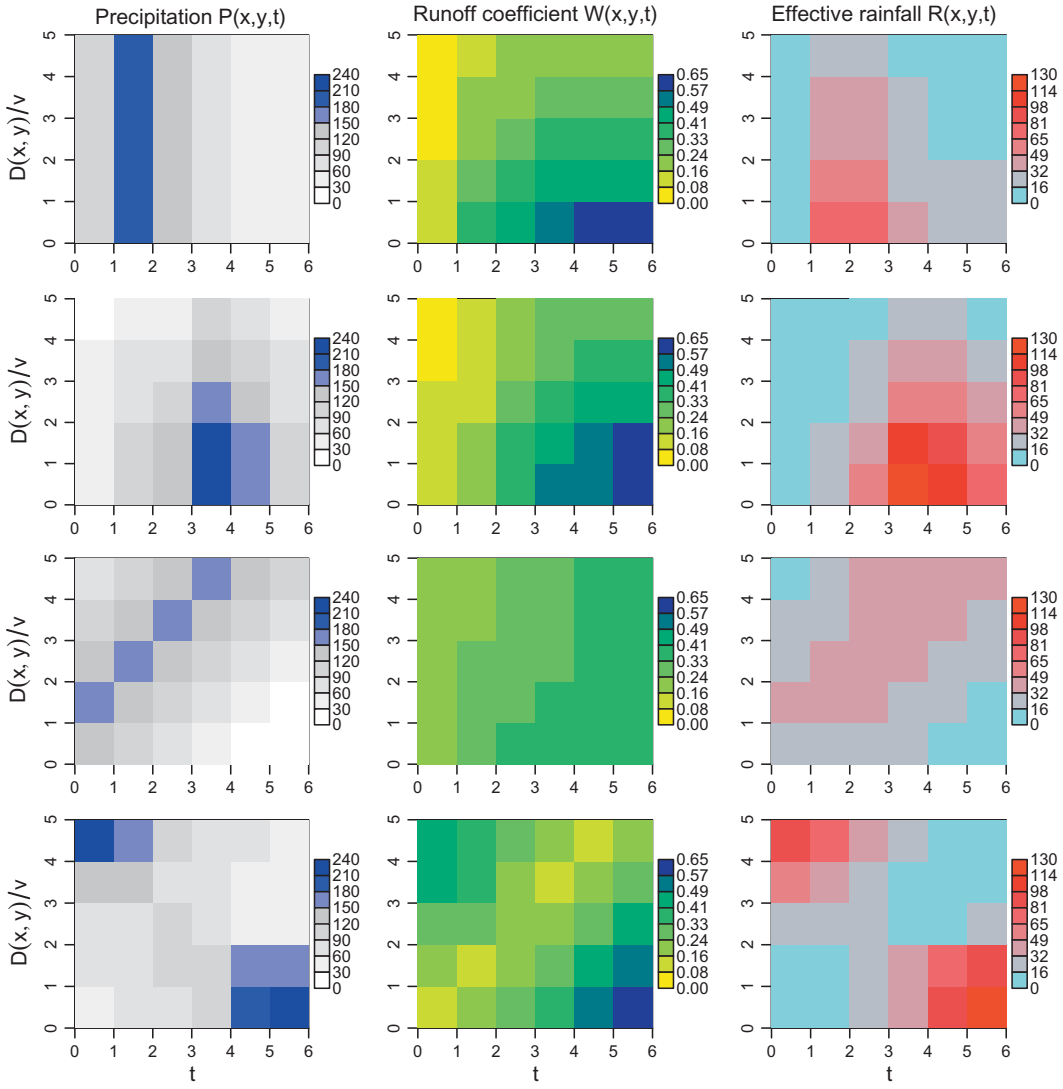

Fig. 2. Four events represented in spatio-temporal diagrams of precipitation ($P(x,y,t)$ [LT^{-1}]), runoff coefficient ($W(x,y,t)$ [·]) and effective rainfall ($R(x,y,t)$ [LT^{-1}]). Proceeding per row: (E1) stationary precipitation uniform in space + stationary runoff coefficient; (E2) stationary precipitation + stationary runoff coefficient; (E3) moving precipitation + stationary runoff coefficient; (E4) double-storm moving precipitation + moving runoff coefficient. Note that both time t and distance to outlet $D(x,y)/v$ are expressed in temporal unit [T].

previous two cases and is more homogeneously distributed in space and time. Also the fourth case (E4) represents a moving storm, which begins upstream and moves downstream. It can be considered as a double event because it is particularly intense at the beginning, then decreases in intensity in the middle part and increases again at the end, when reaching the lower part of the catchment. The runoff coefficient shows a similar behavior, though less pronounced. As a consequence the effective rainfall has also the bimodal shape of the total rainfall, in both time and space.

In the following sections we derive the analytical equations for the instantaneous catchment rainfall excess (the temporal evolution of the spatial average of $R(x,y,t)$), the storm-averaged rainfall excess (the spatial distribution of the temporal average of $R(x,y,t)$) and the storm-averaged catchment rainfall excess (which is essentially the runoff volume). At the same time we provide the results for the sample case study illustrated in Fig. 2.

2.1. Instantaneous catchment rainfall excess

For a catchment with area A, the instantaneous catchment-averaged rainfall excess rate $R_{x,y}(t)$ [LT^{-1}] at time t is

$$R_{x,y}(t) = \frac{1}{A}\int\int_A R(x,y,t)\,dx\,dy$$

and can be expressed in terms of the moments of rainfall P and runoff coefficient W by averaging Eq. (1) over the catchment:

$$R_{x,y}(t) = P_{x,y}(t)\cdot W_{x,y}(t) + \mathrm{cov}_{x,y}(P,W) \tag{2}$$

where

$$P_{x,y}(t) = \frac{1}{A}\int\int_A P(x,y,t)\,dx\,dy$$

is the time series of catchment-averaged rainfall rates [LT^{-1}],

$$W_{x,y}(t) = \frac{1}{A}\int\int_A W(x,y,t)\,dx\,dy$$

is the time series of catchment-averaged runoff coefficient, and

$$\mathrm{cov}_{x,y}(P,W) = \frac{1}{A}\int\int_A [P(x,y,t) - P_{x,y}(t)][W(x,y,t) - W_{x,y}(t)]\,dx\,dy \tag{3}$$

is the time series of the spatial covariance [LT^{-1}] of P and W. Note that, for reasons of space, here and in the remainder of the paper

we use the short notation P, W and R to indicate the local quantities $P(x,y,t)$, $W(x,y,t)$ and $R(x,y,t)$.

From Eq. (2) we see that the catchment-averaged rainfall excess rate at time t ($R_{x,y}(t)$) depends on the catchment-averaged rainfall rate at that time ($P_{x,y}(t)$) and the catchment-averaged runoff generation at the same time ($W_{x,y}(t)$). The catchment-averaged rainfall excess rate also depends on the interactions of space patterns in rainfall and runoff generation: the effect of any correlation between rainfall and runoff generation is explicit in Eq. (2) by the term $\mathrm{cov}_{x,y}(P,W)$. If there is no correlation between the space pattern of the rainfall and the space pattern of the runoff generation process at time t, then the catchment rainfall excess rate at that time is simply the product of the catchment-averaged rainfall rate and catchment-averaged runoff generation. Eq. (2) is a generalisation that does not rely on the separability assumption of Eq. (11) in Woods and Sivapalan (1999).

In Fig. 3 the temporal evolution of the terms in Eq. (2) is shown for the four events of Fig. 2. As already mentioned, the rainfall rate is higher in the first part of the event for the first example (E1) and in the second part for the second example (E2), while the runoff coefficient always increases in time. For the third and fourth examples (E3 and E4) the temporal variability of $P_{x,y}(t)$ is not so pronounced. For the double storm of E4 both $P_{x,y}(t)$ and $W_{x,y}(t)$ have two maximums, at the beginning and at the end of the event.

The graph of the spatial covariances shows that there is no spatial correlation between P and W in E1, which is obvious as the rainfall is uniform in space. In E2, instead, the spatial covariance increases in time and is positive meaning that, especially in the second part of the event, it rains more 'where' the runoff coefficient is high. In E3, $\mathrm{cov}_{x,y}(P,W)$ is instead negative for almost all the event meaning that it rains more where the runoff coefficient is low. The covariance is positive only at the very beginning of the event E3. Actually the storm starts close to the outlet and moves upstream, where the values of W are small. In E4 the covariance is positive and very high at the beginning and at the end of the event, when both precipitation and runoff coefficient are intense.

2.2. Storm-averaged rainfall excess

The time averaged rainfall excess $R_t(x,y)$ [LT^{-1}] at location (x,y) for the period $[0,T_m]$ (where T_m is the storm duration) is given by

$$R_t(x,y) = \frac{1}{T_m}\int_0^{T_m} R(x,y,t)dt$$

and can be expressed in terms of the moments of rainfall P and runoff coefficient W by averaging Eq. (1) over time as

$$R_t(x,y) = P_t(x,y)\cdot W_t(x,y) + \mathrm{cov}_t(P,W) \tag{4}$$

where

$$P_t(x,y) = \frac{1}{T_m}\int_0^{T_m} P(x,y,t)dt$$

is the map of the temporally averaged rainfall rates [LT^{-1}],

$$W_t(x,y) = \frac{1}{T_m}\int_0^{T_m} W(x,y,t)dt$$

is the map of the temporally averaged runoff coefficients, and

$$\mathrm{cov}_t(P,W) = \frac{1}{T_m}\int_0^{T_m} [P(x,y,t)-P_t(x,y)][W(x,y,t)-W_t(x,y)]dt \tag{5}$$

is the map of the temporal covariances [LT^{-1}] of P and W.

While in Eq. (2) runoff generation is integrated in space along the y-axis of the graphs in Fig. 2, in Eq. (4) runoff generation is integrated in time, along the x-axis of the graphs in Fig. 2. The storm-averaged rainfall excess rate at one location ($R_t(x,y)$) depends on the storm-averaged rainfall rate at that location ($P_t(x,y)$) and the storm-averaged runoff generation at the same location ($W_t(x,y)$). The storm-averaged rainfall excess rate also depends on the interactions of temporal shapes in rainfall and runoff generation: the effect of any temporal correlation between rainfall and runoff generation is summarised in the term $\mathrm{cov}_t(P,W)$. If there is no correlation between the temporal evolution of the rainfall and the temporal evolution of the runoff generation process at location (x,y), then the rainfall excess rate in that location is simply the product of the storm-averaged rainfall rate and storm-averaged runoff generation.

Fig. 4 represents the spatial distribution of the terms in Eq. (4) for the four events of Fig. 2. The storm-averaged rainfall $P_t(x,y)$ is uniform in E1, higher close to the outlet in E2, higher upstream in E3 (due to the movement of the storm) and bimodal in E4. In

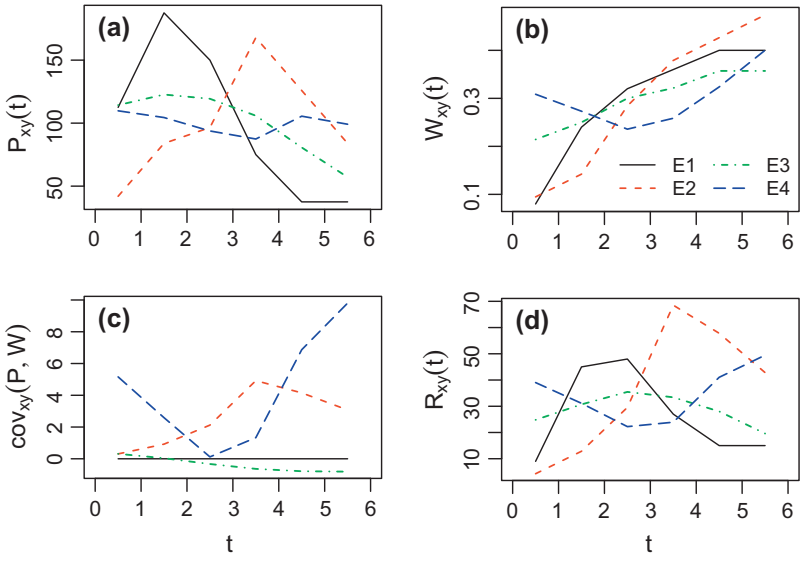

Fig. 3. Temporal evolution of the terms in Eq. (2): (a) catchment-averaged rainfall rate $P_{x,y}(t)$ [LT^{-1}]; (b) catchment-averaged runoff coefficient $W_{x,y}(t)$ [·]; (c) spatial covariance of precipitation and runoff coefficient $\mathrm{cov}_{x,y}(P,W)$ [LT^{-1}]; (d) instantaneous catchment rainfall excess $R_{x,y}(t)$ [LT^{-1}]. The four events of Fig. 2 are considered: (E1) stationary precipitation uniform in space + stationary runoff coefficient; (E2) stationary precipitation + stationary runoff coefficient; (E3) moving precipitation + stationary runoff coefficient; (E4) double-storm moving precipitation + moving runoff coefficient.

all cases the averaged (in time) runoff coefficient is higher close to the catchment outlet. The graph of the temporal covariances shows that $\mathrm{cov}_t(P,W)$ is negative in E1, in particular close to the catchment outlet. This means that it rains 'when' the runoff coefficient is low (in fact it rains more in the first part of the event). In E2, instead, the temporal covariance is positive meaning that, especially close to the catchment outlet, it rains when the runoff coefficient is high (in the second part of the event). The fact that in E3 $\mathrm{cov}_t(P,W)$ is slightly negative is consistent with Fig. 3a, where one sees that the rainfall event is more intense in the first part, when the runoff coefficient is still low. In E4 the covariance is positive and very high close to the outlet and upstream in the catchment, where both precipitation and runoff coefficient are intense.

2.3. Storm-averaged catchment rainfall excess

Eq. (2) provides estimates of rainfall excess at instants in time while Eq. (4) provides estimates of rainfall excess locally in space: estimates of flood volume or effective rainfall require the storm-averaged catchment rainfall excess. The storm-averaged catchment rainfall excess $R_{x,y,t}$ [LT^{-1}] is given by

$$R_{x,y,t} = \frac{1}{T_m}\int_0^{T_m} R_{x,y}(t)dt = \frac{1}{A}\int\int_A R_t(x,y)dx\,dy$$

It can be expressed in terms of the moments of rainfall P and runoff coefficient W as

$$\begin{aligned} R_{x,y,t} &= P_{x,y,t}\cdot W_{x,y,t} + \mathrm{cov}_t(P_{x,y},W_{x,y}) + [\mathrm{cov}_{x,y}(P,W)]_t = \\ &= P_{x,y,t}\cdot W_{x,y,t} + \mathrm{cov}_{x,y}(P_t,W_t) + [\mathrm{cov}_t(P,W)]_{x,y} \end{aligned} \quad (6)$$

where

$$P_{x,y,t} = \frac{1}{T_m}\int_0^{T_m} P_{x,y}(t)dt = \frac{1}{A}\int\int_A P_t(x,y)dx\,dy$$

and

$$W_{x,y,t} = \frac{1}{T_m}\int_0^{T_m} W_{x,y}(t)dt = \frac{1}{A}\int\int_A W_t(x,y)dx\,dy$$

are the time-averaged catchment-averaged rainfall [LT^{-1}] and runoff coefficient [·] values,

$$\mathrm{cov}_t(P_{x,y},W_{x,y}) = \frac{1}{T_m}\int_0^{T_m}[P_{x,y}(t)-P_{x,y,t}][W_{x,y}(t)-W_{x,y,t}]dt \quad (7)$$

is the temporal covariance [LT^{-1}] of the space-averaged P and W,

$$\mathrm{cov}_{x,y}(P_t,W_t) = \frac{1}{A}\int\int_A [P_t(x,y)-P_{x,y,t}][W_t(x,y)-W_{x,y,t}]dx\,dy \quad (8)$$

is the spatial covariance [LT^{-1}] of the time-averaged P and W, and the operators $[\cdot]_t$ and $[\cdot]_{x,y}$ indicate temporal and spatial averages respectively.

One should note that, in general, $[\mathrm{cov}_{x,y}(P,W)]_t \neq \mathrm{cov}_{x,y}(P_t,W_t)$ because the covariance is a non-linear operator, which implies that the mean of covariances is not equal to the covariance of the means. It can be demonstrated (via Appendix A.1) that $[\mathrm{cov}_{x,y}(P,W)]_t - \mathrm{cov}_{x,y}(P_t,W_t) = [\mathrm{cov}_t(P-P_{x,y},W-W_{x,y})]_{x,y}$ (or, equivalently, that $[\mathrm{cov}_t(P,W)]_{x,y} - \mathrm{cov}_t(P_{x,y},W_{x,y}) = [\mathrm{cov}_{x,y}(P-P_t,W-W_t)]_t$), so that Eq. (6) can be rewritten as

$$R_{x,y,t} = \underbrace{P_{x,y,t}\cdot W_{x,y,t}}_{\mathrm{R1}} + \underbrace{\mathrm{cov}_t(P_{x,y},W_{x,y})}_{\mathrm{R2}} + \underbrace{\mathrm{cov}_{x,y}(P_t,W_t)}_{\mathrm{R3}} + \underbrace{[\mathrm{cov}_t(P-P_{x,y},W-W_{x,y})]_{x,y}}_{\mathrm{R4}} \quad (9)$$

Four statistics of the rainfall and runoff generation fields influence the storm runoff of a catchment: (R1) the product of time- and catchment-averaged P and W; (R2) the temporal covariance of the space-averaged P and W; (R3) the spatial covariance of the time-averaged P and W; and (R4) a term that accounts for the spatial variation in temporal covariance (or, equivalently, the temporal variation in spatial covariance). For the special case where P and W are uncorrelated in both space and time, the time-averaged catchment rainfall excess $R_{x,y,t}$ is just the product of the time-averaged catchment rainfall $P_{x,y,t}$ and the time-averaged runoff generation function $W_{x,y,t}$ (i.e., the average fraction of the catchment that is generating runoff). Eq. (9) is a generalisation that does not require the separability assumption of Eq. (12) in Woods and Sivapalan (1999). If this latter is written using the notation of our paper, also Eq. (12) in Woods and Sivapalan (1999) would have four terms, where the fourth of them would be equal to $(\mathrm{cov}_t(P_{x,y},W_{x,y})\cdot\mathrm{cov}_{x,y}(P_t,W_t))/(P_{x,y,t}\cdot W_{x,y,t})$ (see Appendix A.1). Thus the effect of the movement of P and W on the storm-averaged catchment rainfall excess can be isolated as $\mathrm{R4} - \mathrm{R2}\cdot\mathrm{R3}/\mathrm{R1}$.

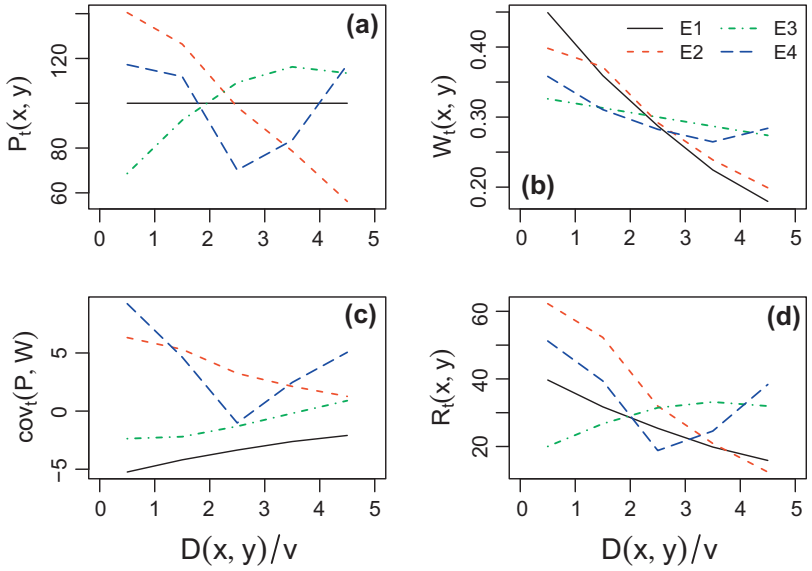

Fig. 4. Spatial distribution of the terms in Eq. (4): (a) storm-averaged local rainfall $P_t(x,y)$ [LT^{-1}]; (b) storm-averaged local runoff coefficient $W_t(x,y)$ [·]; (c) temporal covariance of precipitation and runoff coefficient $\mathrm{cov}_t(P,W)$ [LT^{-1}]; (d) storm-averaged rainfall excess $R_t(x,y)$. Note that distance to outlet $D(x,y)/v$ is expressed in temporal unit [T]. The four events of Fig. 2 are considered: (E1) stationary precipitation uniform in space + stationary runoff coefficient; (E2) stationary precipitation + stationary runoff coefficient; (E3) moving precipitation + stationary runoff coefficient; (E4) double-storm moving precipitation + moving runoff coefficient.

Table 1
Terms of Eq. (9) for the storm averaged catchment rainfall excess [LT^{-1}]. The four events of Fig. 2 are considered: (E1) stationary precipitation uniform in space + stationary runoff coefficient; (E2) stationary precipitation + stationary runoff coefficient; (E3) moving precipitation + stationary runoff coefficient; (E4) double-storm moving precipitation + moving runoff coefficient.

Components of the storm-averaged catchment rainfall excess [LT^{-1}]		E1	E2	E3	E4
R1	$P_{x,y,t} \cdot W_{x,y,t}$	30.00	30.00	30.00	30.00
R2	$\mathrm{cov}_t(P_{x,y}, W_{x,y})$	−3.50	3.39	−0.96	0.15
R3	$\mathrm{cov}_{x,y}(P_t, W_t)$	0	2.32	−0.30	0.39
R4	$[\mathrm{cov}_t(P - P_{x,y}, W - W_{x,y})]_{x,y}$	0	0.26	−0.07	3.92
R4 − R2 · R3/R1	movement	0	0	−0.08	3.92
R1+ . . . +R4	$R_{x,y,t}$	26.50	35.97	28.67	34.47

Table 1 shows the terms of Eq. (9) for the four events of Fig. 2. All the examples have the same $P_{x,y,t}$ and $W_{x,y,t}$, so that the differences in the storm-averaged catchment rainfall excess are due to the spatio-temporal correlations. The temporal covariance $\mathrm{cov}_t(P_{x,y}, W_{x,y})$ is negative in E1 because it rains in the first part of the event, when the runoff coefficient is low, reducing the catchment rainfall excess. In E2 instead, $\mathrm{cov}_t(P_{x,y}, W_{x,y})$ is positive, increasing the overall produced runoff. In this case also the spatial covariance $\mathrm{cov}_{x,y}(P_t, W_t)$ is positive, because it rains close to the outlet, determining a value of $R_{x,y,t}$ which is 20% higher than the product $P_{x,y,t} \cdot W_{x,y,t}$. In this case the spatio-temporal interaction between precipitation and runoff coefficient plays an important role in determining the volume of the flood. In E3 the values of the covariances are both slightly negative meaning that P and W are slightly out-of-phase both in time and in space. For E4 the covariances $\mathrm{cov}_t(P_{x,y}, W_{x,y})$ and $\mathrm{cov}_{x,y}(P_t, W_t)$ are very low but $[\mathrm{cov}_t(P - P_{x,y}, W - W_{x,y})]_{x,y}$ is relatively high (13% of $P_{x,y,t} \cdot W_{x,y,t}$). This is because the spatial and temporal means of P and W are not correlated but, as can be seen in Fig. 3c and Fig. 4c, the temporal and spatial evolutions of the spatial and temporal covariances are significant. In this case, looking at the event E4 from two perspectives, aggregated in time and in space, does not suffice. From Fig. 3a and b one can say that more runoff is generated at the beginning and at the end of the event, when both $P_{x,y}$ and $W_{x,y}$ are high, and from Fig. 4a and b that more runoff is generated close to and far from the outlet, by looking at P_t and W_t. One cannot see, by looking at $P_{x,y}$, $W_{x,y}$, P_t and W_t alone, what is the real joint variability of P and W, evident in Fig. 2, because the spatial and temporal averages mask it. This joint variability can be seen instead looking at $\mathrm{cov}_{x,y}(P,W)$ in Fig. 3c and $\mathrm{cov}_t(P,W)$ in Fig. 4c and is accounted for by the term R4 in Eq. (9). The row R4 − R2 · R3/R1 in Table 1 shows that the increase of runoff production in E4 is indeed due to the movement of P and W. The term accounts for 11% of the flood volume, which is not negligible. In E3, where only P moves, the effect is much less evident.

3. Catchment runoff time

Having estimated in Eqs. (2), (4) and (9) the roles of space and time variability of rainfall and runoff generation in controlling rainfall excess, we now examine the influence of hillslope and channel network routing on the time at which the rainfall excess exits a basin. Water that passes a catchment outlet goes through three successive stages in our framework: (i) the generation of runoff at a point (including waiting for the rain to fall), (ii) hillslope routing, and (iii) channel routing. Each of these stages has an associated "holding time", which is conveniently treated as a random variable (e.g., Rodriguez-Iturbe and Valdes, 1979). Catchment runoff time itself is treated as a random variable (denoted as T_q), which measures the time from the storm beginning until a drop of water exits the catchment. Its distribution [T^{-1}] is given by

$$f_{Tq}(t) = \frac{Q(t)}{\int_0^\infty Q(\tau)d\tau} \tag{10}$$

where $Q(t)$ [LT^{-1}] is the runoff hydrograph. Since the water exiting the catchment has passed in sequence through the three stages mentioned above we can write

$$T_q = T_r + T_h + T_n$$

where T_r, T_h and T_n are the holding times for rainfall excess, hillslope travel and network travel [T].

In the following we derive analytically the mean and variance of T_q, which represent respectively the mean runoff time of the catchment and the dispersion (the inverse of the peakedness) of the hydrograph $Q(t)$. The first moment of the temporal distribution of the flow at the catchment outlet [T] is given by

$$E(T_q) = \frac{\int_0^\infty \tau \cdot Q(\tau)d\tau}{\int_0^\infty Q(\tau)d\tau} \tag{11}$$

while the variance [T^2] is:

$$\mathrm{Var}(T_q) = \frac{\int_0^\infty [\tau - E(T_q)]^2 \cdot Q(\tau)d\tau}{\int_0^\infty Q(\tau)d\tau} \tag{12}$$

Using the mass conservation property (see Appendix A.2) we can write that

$$E(T_q) = E(T_r) + E(T_h) + E(T_n) \tag{13}$$

and that

$$\mathrm{Var}(T_q) = \mathrm{Var}(T_r) + \mathrm{Var}(T_h) + \mathrm{Var}(T_n) + 2\mathrm{Cov}(T_r, T_h) + \\ + 2\mathrm{Cov}(T_r, T_n) + 2\mathrm{Cov}(T_h, T_n) \tag{14}$$

In Woods and Sivapalan (1999), given their assumptions, the variance of T_q could be written as $\mathrm{Var}(T_q) = \mathrm{Var}(T_r) + \mathrm{Var}(T_h) + \mathrm{Var}(T_n)$, where $\mathrm{Var}(T_r)$ contains the temporal variability and $\mathrm{Var}(T_n)$ contains the spatial variability. Here, without the separability assumption and with spatially variable hillslope routing, the variance of T_q also depends on the covariances between times of runoff generation, hillslope routing and channel routing.

3.1. Mean catchment runoff time

The mean catchment runoff time $E(T_q)$ is evaluated from the beginning of the rainfall event. Note that the commonly used "mean catchment response time", i.e., the delay between the centroids of rainfall and runoff, can be calculated subtracting the mean rainfall time from $E(T_q)$. In the following we derive analytically each term of Eq. (13). As in Section 2, we consider the stylised single-stream catchment represented in Fig. 1 to illustrate the method. We assume that the hillslope response times t_h [T], for the five parts of the catchment and for the four events of Fig. 2, are constant in time but vary in space as shown in Fig. 5. In the first example E1 the hillslope response time is uniform in space. In the second and third examples E2 and E3 the upper part of the

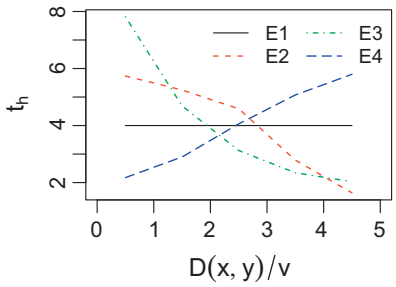

Fig. 5. Spatial distribution of the hillslope travel time t_h [T] for the four events of Fig. 2: (E1) stationary precipitation uniform in space + stationary runoff coefficient; (E2) stationary precipitation + stationary runoff coefficient; (E3) moving precipitation + stationary runoff coefficient; (E4) double-storm moving precipitation + moving runoff coefficient.

catchment responds faster and the lower part slower. In the fourth example E4, on the contrary, the upper part of the catchment responds slower and the lower part faster.

3.1.1. Mean runoff generation time

Rainfall variability can affect the catchment runoff time by both varying the temporal distribution of the rainfall excess (T_r) and the delay due to the flow routing ($T_h + T_n$). To show how the temporal variability of rainfall affects the temporal distribution of rainfall excess, we follow a similar procedure as in Woods and Sivapalan (1999), obtaining (see Appendix A.3):

$$E(T_r) = \underbrace{\frac{T_m}{2}}_{\text{Er1}} + \underbrace{\frac{\text{cov}_t(T, R_{x,y})}{R_{x,y,t}}}_{\text{Er2}} \tag{15}$$

where T_m is the duration of the rainfall event, T is time measured since the start of the rainfall event, $R_{x,y}$ is given by Eq. (2) and $R_{x,y,t}$ is given by Eq. (9). The two terms in Eq. (9) are: (Er1) the midpoint of the rainfall event and (Er2) effects of the temporal variability in rainfall and runoff generation processes, which is an estimate of the time from the middle of the rain event ($T_m/2$) to the centroid of the rainfall excess time series. The second term accounts for the additional runoff time that is caused by the temporal variability in rainfall and runoff generation processes, relative to a rain event that generates rainfall excess at a constant rate throughout the event.

The first three rows in Table 2 show the terms of Eq. (15) for the four events of Fig. 2. All four examples have the same storm duration which gives the same value for $T_m/2$. The temporal variability term (Er2) varies from event to event. For E1 and E3 the term is negative meaning that the centroid of the rainfall excess time series occurs before the middle of the rain event, as can be seen in Fig. 3d. Since the rainfall excess is temporally left skewed, the average rainfall excess time is smaller than that of a rain event that generates rainfall excess at a constant rate throughout the event. On the contrary, for E2 and E4 the temporal variability term is positive because the rainfall excess is (temporally) concentrated in the second part of the event (see Fig. 3d).

3.1.2. Mean hillslope travel time

Following a similar reasoning (Appendix A.3) we can express the delay of the hillslope routing as

$$E(T_h) = [\theta_h]_{x,y,t} + \frac{[\text{cov}_t(\theta_h, R)]_{x,y}}{R_{x,y,t}} + \frac{\text{cov}_{x,y}([\theta_h]_t, R_t)}{R_{x,y,t}} \tag{16}$$

where $\theta_h(x,y,t)$ [T] is the delay with which the rainfall excess generated at location (x,y) and at the time-step t is routed to the channel network. The three terms in Eq. (16) are: (i) average hillslope travel time, i.e., the average time taken for rainfall excess to travel from a location where rainfall excess was generated to the base of the hillslope; (ii) temporal variability term related to the hillslope routing, which accounts for the correlation between the temporal pattern of runoff generation and the temporal evolution of the hillslope response at different locations; (iii) space variability term related to the hillslope routing, which accounts for the correlation between the spatial pattern of runoff generation and of the time-averaged hillslope response.

Here we assume that the hillslope routing time $t_h(x,y)$ is constant in time but varies in space, then:

$$E(T_h) = \underbrace{[t_h]_{x,y}}_{\text{Eh1}} + \underbrace{\frac{\text{cov}_{x,y}(t_h, R_t)}{R_{x,y,t}}}_{\text{Eh2}} \tag{17}$$

where the first term (Eh1) is the spatially-averaged hillslope travel time and the second space variability term (Eh2) accounts for the additional hillslope-routing time that is caused by the spatial variability in rainfall excess, relative to a rain event that generates rainfall excess uniformly over the catchment. If, as in Woods and Sivapalan (1999), we assume that the hillslope response can be modeled as a linear reservoir with response time $t_h(x,y)$ constant in time, then $[\theta_h(x,y,t)]_t = t_h(x,y)$ and Eq. (17) is still valid. If t_h is invariant also in space, as in Woods and Sivapalan (1999), then $E(T_h) = t_h$.

Rows 4–6 in Table 2 show the terms of Eq. (17) for the four events of Fig. 2. All four examples have the same mean hillslope routing time $[t_h]_{x,y}$. The spatial variability term is instead different.

Table 2
Mean rainfall excess time $E(T_r)$, mean hillslope response time $E(T_h)$, mean network response time $E(T_n)$ and mean catchment runoff time $E(T_q)$ (Eq. (13)). The terms in Eqs. (15), (17) and (19) are also shown. All terms are expressed in temporal unit [T]. The four events of Fig. 2 are considered: (E1) stationary precipitation uniform in space + stationary runoff coefficient; (E2) stationary precipitation + stationary runoff coefficient; (E3) moving precipitation + stationary runoff coefficient; (E4) double-storm moving precipitation + moving runoff coefficient.

Components of the mean catchment runoff time [T]		E1	E2	E3	E4
Runoff generation					
Er1	$T_m/2$	3.00	3.00	3.00	3.00
Er2	Temporal variability of $R_{x,y}$	−0.25	0.85	−0.11	0.20
Er1 + Er2	$E(T_r)$	2.75	3.85	2.89	3.20
Hillslope routing					
Eh1	$[t_h]_{x,y}$	4.00	4.00	4.00	4.00
Eh2	Spatial variability of t_h vs. R_t	0	0.76	−0.35	−0.24
Eh1 + Eh2	$E(T_h)$	4.00	4.76	3.65	3.76
Channel routing					
En1	$D_{x,y}/v$	2.50	2.50	2.50	2.50
En2	Spatial variability of D vs. R_t	−0.45	−0.73	0.21	−0.24
En1 + En2	$E(T_n)$	2.05	1.77	2.71	2.26
Er1 + … + En2	$E(T_q)$	8.80	10.39	9.25	9.23

In E1 it is 0 because t_h does not vary in space, as shown in Fig. 5. For E2 and E3 the spatial variability term assumes positive and negative values respectively, even though in both cases t_h is inversely proportional to the distance to the outlet (see Fig. 5). This is because in the second example $R_t(x,y)$ is higher close to the outlet (as t_h) while it is lower in the third example (see Fig. 4d). For E4 the hillslope travel time t_h is higher far from the outlet where the effective rainfall is lower, so that the covariance is slightly negative. In E2 the catchment runoff time is retarded because the runoff is produced mainly where the hillslope travel time is high, while the opposite holds for E3 and E4. In event E2, the spatial variability term Eh2 causes the 16% of the mean hillslope response time, which demonstrates the importance of accounting for the spatial variability of hillslope routing.

3.1.3. Mean network travel time

Analogously to Eq. (16), the delay of the channel routing can be derived as

$$E(T_n) = [\theta_n]_{x,y,t} + \frac{[\mathrm{cov}_t(\theta_n, R)]_{x,y}}{R_{x,y,t}} + \frac{\mathrm{cov}_{x,y}([\theta_n]_t, R_t)}{R_{x,y,t}} \quad (18)$$

where $\theta_n(x,y,t)$ [T] is the delay with which the rainfall excess generated at location (x,y) and at the time-step t, once entered the channel network, is routed to the outlet of the catchment (see Appendix A.3). It has been shown that for a given pattern of flow paths across the catchment, it is always possible to find a single value of flow celerity v such as the mean travel time across the entire catchment and therefore the catchment response time is unchanged (Robinson et al., 1995; Saco and Kumar, 2002; D'Odorico and Rigon, 2003). Therefore, given $D(x,y)$ as the spatial pattern of flow distances to the catchment outlet, we have that $\theta_n(x,y) = D(x,y)/v$ and Eq. (18) simplifies to

$$E(T_n) = \underbrace{\frac{D_{x,y}}{v}}_{\mathrm{En1}} + \underbrace{\frac{\mathrm{cov}_{x,y}(D, R_t)}{v \cdot R_{x,y,t}}}_{\mathrm{En2}} \quad (19)$$

The two terms in Eq. (19) are: (En1) average travel time in the channel network; (En2) space variability term related to the channel routing, which is the distance from the centroid of the catchment to the centroid of the rainfall excess pattern. The second term in Eq. (19) accounts for the additional channel-routing time that is caused by the spatial variability in rainfall excess, relative to a rain event that generates rainfall excess uniformly over the catchment.

Rows 7–9 in Table 2 show the terms of Eq. (19) for the four events of Fig. 2. All four examples have the same mean channel routing time $D_{x,y}/v$. The spatial variability term is instead different. In E1, E2 and E4 it is negative because the runoff is generated mainly close to the catchment outlet, as can be seen in Fig. 4d. This reduces the catchment runoff time in comparison to a rain event that generates rainfall excess uniformly over the catchment. In E3 the catchment runoff time is retarded because the runoff is produced mainly far from the catchment outlet (see Fig. 4d).

3.2. Variance of catchment runoff time

In the following we derive analytically each term of Eq. (14) and illustrate the equations using the storm events of Fig. 2 affecting the stylised single-stream catchment represented in Fig. 1.

3.2.1. Variance of runoff generation time

The variance of the time of rainfall excess is (see Appendix A.4):

$$\mathrm{Var}(T_r) = \underbrace{\frac{T_m^2}{12}}_{\mathrm{Vr1}} + \underbrace{\frac{\mathrm{cov}_t[T^2, R_{x,y}(T)]}{R_{x,y,t}} - \frac{\mathrm{cov}_t[T, R_{x,y}(T)]}{R_{x,y,t}}\left[T_m + \frac{\mathrm{cov}_t[T, R_{x,y}(T)]}{R_{x,y,t}}\right]}_{\mathrm{Vr2}} \quad (20)$$

The two terms in Eq. (20) are: (Vr1) variance of the rainfall excess time series as if it was steady throughout the event (i.e., longer rain events cause greater variance in runoff time, and therefore more dispersed hydrographs, than short rain events, other conditions being equal); (Vr2) additional variance in the rainfall excess time series that is caused by the temporal variability in rainfall and runoff generation processes, relative to a rain event that generates rainfall excess at a constant rate throughout the event. This second term can be negative, signifying that the patterns of rainfall excess have concentrated the catchment response in time. To take an extreme example, if 99% of the rain falls in just 1 h of a 10-h event, then $T_m^2/12$ would be a gross overestimate of the variance of time of rainfall excess and the term Vr2 in Eq. (20) (which accounts for the temporal peakedness of rainfall) will provide the required correction.

Table 3
Variance of the rainfall excess time $\mathrm{Var}(T_r)$, variance of the hillslope response time $\mathrm{Var}(T_h)$, variance of the network response time $\mathrm{Var}(T_n)$, covariances between T_r, T_h and T_n and variance of the catchment runoff time $\mathrm{Var}(T_q)$ (Eq. (14)). The terms in Eqs. (20), (21), (23), (24), (25) and (26) are also shown. All terms are expressed in squared temporal unit [T^2]. The four events of Fig. 2 are considered: (E1) stationary precipitation uniform in space + stationary runoff coefficient; (E2) stationary precipitation + stationary runoff coefficient; (E3) moving precipitation + stationary runoff coefficient; (E4) double-storm moving precipitation + moving runoff coefficient.

Components of variance of the catchment runoff time [T^2]		E1	E2	E3	E4
Runoff generation					
Vr1	$T_m^2/12$	3.00	3.00	3.00	3.00
Vr2	Temporal variability of $R_{x,y}$	−1.07	−1.42	−0.45	0.56
Vr1 + Vr2	$\mathrm{Var}(T_r)$	1.93	1.58	2.55	3.56
Hillslope routing					
Vh1	$\mathrm{var}_{x,y}(t_h)$	0	2.39	4.48	1.79
Vh2	Spatial variability of t_h vs. R_t	0	−0.86	−0.82	0.31
Vh1 + Vh2	$\mathrm{Var}(T_h)$	0	1.53	3.66	2.10
Channel routing					
Vn1	$\mathrm{var}_{x,y}(D)/v^2$	2.08	2.08	2.08	2.08
Vn2	Spatial variability of D vs. R_t	−0.14	−0.46	−0.18	0.39
Vn1 + Vn2	$\mathrm{Var}(T_n)$	1.95	1.62	1.91	2.48
Covariances					
2 Crh	$2\mathrm{Cov}(T_r, T_h)$	0	0	−1.53	−3.34
2 Crn	$2\mathrm{Cov}(T_r, T_n)$	0	0	1.17	−3.52
2 Chn1	$2\mathrm{cov}_{x,y}(t_h, D)$	0	−4.26	−5.56	3.77
2 Chn2	Spatial variability of t_h vs. D vs. R_t	0	1.31	0.80	0.70
2 (Chn1 + Chn2)	$2\mathrm{Cov}(T_h, T_n)$	0	−2.95	−4.76	4.47
Vr1+...+2 Chn2	$\mathrm{Var}(T_q)$	3.88	1.78	3.00	5.75

The first three rows in Table 3 show the terms of Eq. (20) for the four events of Fig. 2. All four examples have the same storm duration which gives the same value for $T_m^2/12$. The temporal variability term Vr2 is instead different. In the first three examples (E1, E2 and E3) it is negative meaning that the shape of $R_{x,y}(t)$ is responsible for the peakedness of the hydrograph. Not surprisingly E2, with the most peaky instantaneous catchment rainfall excess (see Fig. 3d), has the lowest value of $\mathrm{Var}(T_r)$ while E3, with the smoothest $R_{x,y}(t)$, has a higher value of $\mathrm{Var}(T_r)$. Event E4 has a positive temporal variability term Vr2, due to the fact that it is a double event. Effective rainfall is high at the beginning and at the end of the event and low in the central part. This causes the variance in the rainfall excess time series to be higher than the variance that a rain event, which generates rainfall excess at a constant rate throughout the event, would have produced.

3.2.2. Variance of hillslope travel time

If we assume that the hillslope routing time $t_h(x,y)$ is constant in time but varies in space, then the variance of the delay of the hillslope routing is derived (Appendix A.4) as

$$\mathrm{Var}(T_h) = \underbrace{\mathrm{var}_{x,y}(t_h)}_{\mathrm{Vh1}} + \underbrace{\frac{\mathrm{cov}_{x,y}[t_h^2, R_t]}{R_{x,y,t}} - \frac{\mathrm{cov}_{x,y}[t_h, R_t]}{R_{x,y,t}} \cdot \left[2[t_h]_{x,y} + \frac{\mathrm{cov}_{x,y}[t_h, R_t]}{R_{x,y,t}}\right]}_{\mathrm{Vh2}} \tag{21}$$

The two terms in Eq. (21) are: (Vh1) spatial variance of the hillslope routing time; (Vh2) additional variance in hillslope routing time that is caused by the spatial variability in rainfall excess, relative to a rain event that generates rainfall excess uniformly throughout the basin. This second term can be negative, signifying that the patterns of rainfall excess have concentrated the catchment response in space. If most of the rainfall excess was generated where the hillslope response time is much faster (or much slower) than in the rest of the catchment, then the spatial variance of t_h would be a poor estimate of the variance of effective hillslope routing time and the term Vh2 of Eq. (21) (spatial covariance term) would provide the necessary correction.

If, as in Woods and Sivapalan (1999), we were to assume that the hillslope routing can be modeled as a linear reservoir with response time $t_h(x,y)$, the variance of the delay of the hillslope routing would be different and would read (see Appendix A.4)

$$\mathrm{Var}(T_h) = [t_h^2]_{x,y} + \mathrm{var}_{x,y}(t_h) + 2\frac{\mathrm{cov}_{x,y}[t_h^2, R_t]}{R_{x,y,t}} - \frac{\mathrm{cov}_{x,y}[t_h, R_t]}{R_{x,y,t}} \cdot \left[2[t_h]_{x,y} + \frac{\mathrm{cov}_{x,y}[t_h, R_t]}{R_{x,y,t}}\right] \tag{22}$$

In the space-invariant linear reservoir case of Woods and Sivapalan (1999), $\mathrm{Var}(T_h) = t_h^2$. In our examples here, we refer to Eq. (21) meaning that the hillslope routing is instantaneous after the delay t_h, so that in the space-invariant case $\mathrm{Var}(T_h) = 0$.

Rows 4–6 in Table 3 show the terms of Eq. (21) for the four events of Fig. 2. In E1 both terms are equal to 0 because t_h is uniform in the catchment. E3 has the highest value of $\mathrm{var}_{x,y}(t_h)$, which can be derived from Fig. 5 and implies a more dispersed hydrograph. In both E2 and E3 the spatial variability term Vh2 is negative, meaning the spatial variability in rainfall excess causes a smaller variance of the hydrograph if compared to a rain event that generates rainfall excess uniformly throughout the basin. In E2 the runoff is mainly produced on slow responding hillslopes, while in E3 it is mainly produced on fast responding hillslopes. In both cases this has the effect of concentrating runoff even if, as shown in Table 2, runoff is delayed for E2 and advanced for E3, compared to a rain event that generates rainfall excess uniformly throughout the basin. Once more, E4 is distinctive, having a positive spatial variability term Vh2. In this case, $R_t(x,y)$ is bimodal while $t_h(x,y)$ is monotonic (as T in Eq. (20)). Runoff is produced more on fast and slow responding hillslopes and less on hillslopes with average t_h, thus determining a variance in hillslope routing time bigger than the variance that would result from a rain event that generates rainfall excess uniformly throughout the basin.

3.2.3. Variance of network travel time

The variance of the delay of the channel routing is

$$\mathrm{Var}(T_n) = \underbrace{\frac{\mathrm{var}_{x,y}(D)}{v^2}}_{\mathrm{Vn1}} + \underbrace{\frac{\mathrm{cov}_{x,y}[D^2, R_t]}{v^2 R_{x,y,t}} - \frac{\mathrm{cov}_{x,y}[D, R_t]}{v R_{x,y,t}} \cdot \left[2\frac{D_{x,y}}{v} + \frac{\mathrm{cov}_{x,y}[D, R_t]}{v R_{x,y,t}}\right]}_{\mathrm{Vn2}} \tag{23}$$

The two terms in Eq. (23) are: (Vn1) variance of travel time in the channel network, thus a catchment with a wide range of flow distances to the outlet is predicted to have a large variance in runoff time (see Rinaldo et al., 1991); (Vn2) additional variance in channel-routing time that is caused by the spatial variability in rainfall excess, relative to a rain event that generates rainfall excess uniformly throughout the basin. This second term can be negative, signifying that the patterns of rainfall excess have concentrated the catchment response in space. Again, to take an extreme example, if 99% of the rainfall excess was generated within a single 1-h isochrone, then the variance of flow distance would be a poor estimate of the variance of effective flow distance and the term Vn2 of Eq. (23) (flow distance covariance) would provide the necessary correction.

Rows 7–9 in Table 3 show the terms of Eq. (23) for the four events of Fig. 2. All four examples have the same variance for the channel routing time $\mathrm{var}_{x,y}(D)/v^2$. The spatial variability term Vn2 varies between events. In E1, E2 and E3 it is negative meaning that the spatial pattern of $R_{x,y}(t)$ is responsible for the hydrograph being more peaky relative to a rain event that generates rainfall excess uniformly throughout the basin. Not surprisingly E2, where the rainfall excess is more concentrated in space (see Fig. 4d), has the lowest value of $\mathrm{Var}(T_n)$ while E1 and E3, with similarly smoother $R_t(x,y)$, have higher $\mathrm{Var}(T_n)$. Once again, E4 is distinctive, having a positive spatial variability term. The fourth example is a double-peaked storm both in time and space. The fact that $R_t(x,y)$ is bimodal, with high values close and far from the outlet, causes a variance in channel routing time bigger than the variance that would result from a rain event that generates rainfall excess uniformly throughout the basin.

3.2.4. Covariances of runoff generation time with hillslope and network travel times

The additional terms $\mathrm{Cov}(T_r, T_h)$ and $\mathrm{Cov}(T_r, T_n)$ in Eq. (14) are the covariance terms that arise from the relaxation of the hypothesis of stationarity of the produced runoff over the catchment (the separability assumption in Woods and Sivapalan, 1999). The covariance between rainfall excess time and hillslope-routing time $\mathrm{Cov}(T_r, T_h)$ accounts for the additional variance of the runoff time because of the correlation between time of runoff production and the spatial variability of hillslope response time. As derived in Appendix A.5, this covariance can be written as:

$$\mathrm{Cov}(T_r, T_h) = \underbrace{\frac{\mathrm{cov}_t[T,\ \mathrm{cov}_{x,y}(t_h, R)]}{R_{x,y,t}} - \frac{\mathrm{cov}_t(T, R_{x,y})}{R_{x,y,t}} \cdot \frac{\mathrm{cov}_{x,y}(t_h, R_t)}{R_{x,y,t}}}_{\mathrm{Crh}} \tag{24}$$

The first term represents how much the covariance between runoff generation and hillslope routing time varies in time. This could be non-zero also without movement of the storm, just because of independent spatial and temporal variabilities. The second term in Eq. (24) removes the amount of correlation between runoff generation and hillslope routing time that is due to spatial and temporal

variabilities considered independently. As a result, the difference of the two terms is the covariance of time, runoff generation and hillslope response time due to the movement of runoff generation only.

Analogously, the covariance between rainfall excess time and network routing time $\mathrm{Cov}(T_r,T_n)$, which accounts for the additional variance of the runoff time because of the correlation between time runoff production and the time in the channel network, can be written as:

$$\mathrm{Cov}(T_r,T_n)=\underbrace{\frac{\mathrm{cov}_t[T,\mathrm{cov}_{x,y}(D,R)]}{vR_{x,y,t}}-\frac{\mathrm{cov}_t(T,R_{x,y})}{R_{x,y,t}}\cdot\frac{\mathrm{cov}_{x,y}(D,R_t)}{vR_{x,y,t}}}_{\mathrm{Crn}} \quad (25)$$

The first term represents how much the correlation between runoff generation and distance to the outlet varies in time. It is a measure of the spatio-temporal variability due to correlation of runoff generation, distance to the outlet and time. The second term removes the amount of correlation between runoff generation and distance to the outlet that is due to spatial and temporal variabilities considered independently. As a result the difference of the two terms is the covariance of runoff generation, distance to the outlet and time due to the movement of runoff generation only.

In Rows 10–11 in Table 3 the values of $\mathrm{Cov}(T_r,T_h)$ and $\mathrm{Cov}(T_r,T_n)$ are shown for the four events of Fig. 2. The first two events are stationary and, therefore, have the two terms equal to 0. In the third example $\mathrm{Cov}(T_r,T_h)$ is negative while $\mathrm{Cov}(T_r,T_n)$ is positive. This is the effect of the rainfall moving upstream. From the point of view of the network routing, it is obvious that a storm moving from the catchment outlet upstream would produce a smoother hydrograph than in the opposite case (smoother also than a similar event, which produces runoff in the same parts of the catchment, with a similar overall temporal evolution, but which does not move). The peakedness of the hydrograph is instead increased because the rainfall starts where the hillslope routing is slow and moves towards the fast responding hillslopes, thus determining a negative $\mathrm{Cov}(T_r,T_h)$. For E4, instead, both the covariance terms are highly negative: $\mathrm{Cov}(T_r,T_n)$ is negative because the storm moves towards the catchment outlet, thus concentrating the hydrograph in time; $\mathrm{Cov}(T_r,T_h)$ is negative because the storm moves towards fast responding hillslopes.

3.2.5. Covariance between hillslope and network travel times

The last term $\mathrm{Cov}(T_h,T_n)$ of Eq. (14) arises from the relaxation of constant hillslope routing in the catchment, as made by Woods and Sivapalan (1999). The covariance between hillslope-routing time and channel-routing time accounts for the additional variance of the runoff time because of the spatial correlation between hillslope response time and the time in the channel network. As derived in Appendix A.5, this covariance can be written as:

$$\mathrm{Cov}(T_h,T_n)=\underbrace{\frac{\mathrm{cov}_{x,y}(t_h,D)}{v}}_{\mathrm{Chn1}}+\underbrace{\frac{\mathrm{cov}_{x,y}(t_h\cdot D,R_t)}{vR_{x,y,t}}-[t_h]_{x,y}\frac{\mathrm{cov}_{x,y}(D,R_t)}{vR_{x,y,t}}+}_{\mathrm{Chn2}}$$
$$\underbrace{-\frac{D_{x,y}}{v}\frac{\mathrm{cov}_{x,y}(t_h,R_t)}{R_{x,y,t}}-\frac{\mathrm{cov}_{x,y}(D,R_t)}{vR_{x,y,t}}\cdot\frac{\mathrm{cov}_{x,y}(t_h,R_t)}{R_{x,y,t}}}_{\mathrm{Chn2}} \quad (26)$$

The first term Chn1 is the spatial covariance between hillslope routing time and distance to the outlet, which can be considered as a characteristic of the catchment structure: it is positive if the hillslopes respond fast close to the outlet and slow far from the outlet, smoothing the catchment response if the rainfall excess is uniform; if the hillslopes respond fast far from the outlet and slow close to it, the catchment response to uniform rainfall excess is concentrated in time and the term is negative. The spatial variability of the rainfall excess is accounted for in the second term Chn2, which measures the joint correlation of $t_h(x,y)$, $D(x,y)$ and $R_t(x,y)$. These terms describe how the rainfall excess is spatially organised with respect to the hillslope and network spatial structure.

In Rows 12–14 of Table 3 the values of $\mathrm{Cov}(T_h,T_n)$ are shown for the four events of Fig. 2. Thus, the first term is event independent, while the other terms are event dependent. For E1, obviously, the term is equal to 0 because t_h is constant in space. For E2, E3 and E4, the event dependent terms explain as whole from 15% to 30% of the total $\mathrm{Cov}(T_h,T_n)$, whose sign is essentially controlled by the first term, event independent. In E2 and E3 the covariance Chn1 is negative because t_h and D are negatively correlated. The term Chn2 is significant in E2 and has a positive value because runoff is produced mainly close to the outlet, so that the negative correlation between t_h and D is less effective than in the case of a rain event that generates rainfall excess uniformly throughout the basin. Therefore $|\mathrm{Cov}(T_h,T_n)|<|\mathrm{cov}_{x,y}(t_h,D/v)|$. In E4, instead, both terms are positive because t_h and D are positively correlated and runoff is generated both upstream (where t_h is high) and downstream (where t_h is low).

4. Discussion

We propose a general analytical framework for exploring the dependence of the catchment flood event response characteristics on the spatial and temporal variability of the rainfall patterns, runoff generation and runoff routing across the hillslope and channel network. The catchment response characteristics analysed are: the average rainfall excess rate (Eq. (9)), which multiplied by the storm duration is the flood volume; the mean catchment runoff time (Eq. (13)), which is a surrogate for the time to peak; the variance of runoff time (Eq. (14)), which together with the storm-averaged catchment rainfall excess is indicative of the magnitude of the peak runoff. Of course one could run a model which has the same assumptions of the framework and calculate the flood hydrograph in a straightforward way. For example, Fig. 6 shows the hydrographs produced by the four events of Fig. 2. Eqs. (9), (13) and (14) give the second order moments that approximate these hydrographs. If one were interested in fully representing the hydrographs, one would also have to consider the higher order moments. However the most important hydrological characteristics are indeed captured by the framework. From Table 1 one can see that E2 is the event with maximum volume while E1 is the smallest. From Table 2 one sees that the peak in E2 is more delayed than the others and from Table 3 that E2 has the highest peak while E4 produces the most dispersed hydrograph. All this information is explicitly shown in Fig. 6. What Fig. 6 does not tell but Tables 1, 2 and 3 do, is the quantitative contribution of the different processes in determining volume, position and spread of the hydrographs. In the tables and in the equations, each of the three

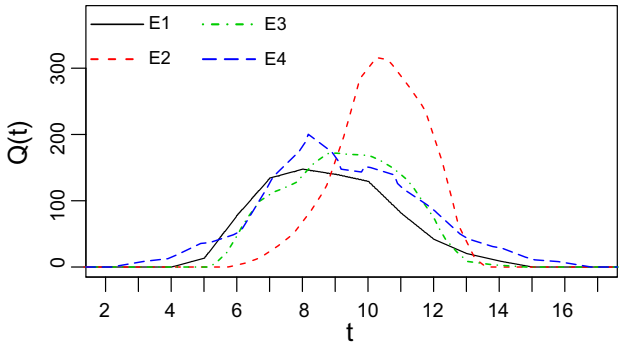

Fig. 6. Hydrographs $Q(t)$ [LT^{-1}] produced by the four events of Fig. 2. The analytical framework proposed here gives the moments of these hydrographs and the magnitude of the process components.

catchment response characteristics (runoff generation, hillslope and channel routing) is disaggregated in two classes of components: the first explained by the catchment average values, the second explained by the spatial and temporal variability of the key variables. This second class of components is expressed by a set of spatial and temporal covariances. Thus, the effect of the spatial and temporal variability is described by the dynamic interaction in space and time among the key variables.

The average rainfall excess rate is expressed by the product of the mean rainfall with the mean runoff coefficient plus a set of three covariances describing how the rainfall varies in time and space with respect to the dynamic evolution of the runoff coefficient. In the examples, E2 has the biggest volume because it rains when and where the runoff coefficient is high (see the terms R2 and R3 in Table 1). In E1, instead, rainfall and runoff coefficient are negatively correlated in time. In E4, finally, what is important is the movement of the storm and of the runoff coefficient.

The magnitude of the covariance terms in Table 1 are significantly dependent on the dominant runoff generation mechanisms. If infiltration excess is dominant, the runoff coefficient is significantly affected by local rainfall intensity and we should expect a high positive temporal covariance between rainfall and runoff coefficient (terms R2 and R4 in Eq. (9)). The spatial structure of the time-average runoff coefficient should be strongly dependent on the spatial pattern of rainfall intensity above higher threshold values and on the local properties affecting infiltration excess (soil properties, vegetation, antecedent conditions, etc.). For rainfall events with high intensity for the entire rainfall event and across the entire catchment, with uniform properties, all covariance terms (R2 to R4) are expected to be positive.

If saturation excess is dominant, the space–time evolution of the runoff coefficient is mainly controlled by catchment features at larger spatial scales. When considering many events, on average, R3 and R4 are expected to be null, unless rainfall is structured according to the function controlling the spatial distribution of the runoff coefficient. This corresponds to the case reported in Winchell et al. (1998), who explored the sensitivity of the simulated runoff to the spatial and temporal variability of the rainfall by running some numerical experiments with TOPMODEL. These results can be explained by the fact that TOPMODEL defines the patterns of the runoff coefficient by scaling its average value by a function of the wetness index, thus R3 and R4 can be significant only if rainfall shows some correlation with the wetness index. Previous studies have shown that the effects of spatial variability of rainfall on the storm flow volume can be large when infiltration excess is the dominant runoff generation mechanism (Krajewski et al., 1991; Loague, 1988; Michaud and Sorooshian, 1994; Ogden and Julien, 1994; Winchell et al., 1998), while they are negligible when saturation excess is dominant (Loague, 1988; Obled et al., 1994; Shah et al., 1996a,b; Winchell et al., 1998). Within the proposed general framework, these results can be interpreted by evaluating the space–time covariance between the runoff coefficient and the rainfall patterns.

In our framework, the first and the second temporal moments of the hydrograph are expressed by event and catchment characteristic time-scales, considered independently, plus a set of spatial and temporal covariances representing how the generated rainfall excess is spatially and temporally structured with respect to the spatial organisation of the contributing hillslopes and network, each characterised by a specific travel time. We explicitly describe how the first and second temporal moments of the hydrograph can be affected by the spatial distribution of the runoff generation. This finding is consistent with Naden (1992), who suggested weighting the flow distance with the effective rainfall in order to incorporate the effect of the spatial variability into a unit hydrograph flood type estimation procedure. The analytical expressions also explicitly describe the role of the correlation between the rainfall excess patterns and the spatial structure of the hillslope and river network. For example, despite the fact that it mainly rains close to the catchment outlet (term En2 in Table 2), event E2 gives the most delayed peak because the main rainfall burst occurs temporally in the second part of the event and where the hillslope routing is slow (terms Er2 and Eh2). The greater peakedness of the hydrograph in E2 follows from the temporal peakedness of runoff generation (term Vr2 in Table 3), from the concentration in space (which determines terms Vh2 and Vn2) and because hillslope routing and channel routing are negatively correlated in space (term 2 Chn1). Similar aspects have been explored by Nicótina et al. (2008) by using a random space sampling strategy, to shed lights into the influence exerted by space–time rainfall patterns on hydrograph shapes as simulated with a distributed model. Terms similar to En2 and Vn2 were used by Sangati et al. (2009) in the analysis of the effect of coarsening the spatial rainfall variability on flood modelling. Also, in a regional analysis of storm hydrographs, Di Lazzaro (2009) has adopted analytical expressions to determine the first and second moment of the Width Function based Instantaneous Unit Hydrograph taking into account the statistical dependence between hillslope and channel lengths.

The effect of storm motion on flood peaks has been studied in a model-based investigation by Ogden et al. (1995), who showed how the maximum enhancement of flood peak occurs when the storm motion is downslope and at the same speed as the flood wave. In our more general analytical framework, we express this result as a direct consequence of the negative covariance between the runoff generation time and the flow distance ($\mathrm{Cov}(T_r, T_n) < 0$), thus reducing the temporal variance of catchment runoff time (Eq. (25)), i.e., concentrating the hydrograph in time and increasing the magnitude of the peak. This effect is evident in event E4 (term 2 Crn in Table 3). Our framework also accounts for the interaction of storm motion with the spatial distribution of hillslopes through term 2 Crh. In event E4 this effect is as important as the correlation with channel flow distance and the sum of 2 Crh and 2 Crn has the effect of doubling the peak (i.e., without storm motion $\mathrm{Var}(T_q)$ would have been of the order of 12 instead of 6). In E3, instead, the effect of storm motion does not influence the spread of the hydrograph because 2 Crh and 2 Crn compensate each other.

Although this paper removes some significant limitations of the Woods and Sivapalan (1999) analytical framework, so that moving storms and spatially variable hillslope response are now included, there are still a number of assumptions constraining the underlying theory and its application. Run-on infiltration processes are neglected, i.e., rainfall excess is routed to the outlet without any infiltration loss along its paths to the outlet. This hypothesis is generally applicable at the event scale during wetter periods, when the connectivity of the soil moisture patterns is sufficiently developed (Western et al., 2001). The hillslope is taken as elemental routing unit of the catchment, through which rainfall excess is routed to the catchment outlet according to an independent, but time-varying delay. Channel velocity is assumed constant in space and time. These assumptions are consistent with the majority of the hydrological models currently applied for predicting catchment flood response. Ultimately, we believe that it is not worth relaxing them, given the aim of easily interpreting and comparing the process components of flood response. The analytical framework proposed in this paper is not intended to be a predictive model but a tool to explicitly quantify the space–time interactions between rainfall and catchment state during flood events. It should be noted that we are interested in the event scale, therefore it is important to define what flood events are. If one extends the time period of the analysis so that it includes a large number of zero rainfall intervals, then the framework is no longer relevant because it only addresses single event flood response, but the hydrological phenomena of most

interest when one has mostly zero rainfall are not floods, but other processes, such as evaporation and gradual subsurface flow.

The theoretical value of the framework is in its coherence and simplicity. The proposed equations parsimoniously give the order of magnitude of process involved in catchment flood response in a similar way as in fluid dynamics the St. Venant equations can be used to provide insight into the open channel flow motion. We believe that the framework developed here has also an important practical value. Despite the apparently complex analytical structure, it can be easily applied, once the space–time structure of the key variables is provided. It is important to note that patterns of runoff coefficient are required for applying this analytical framework to real catchments. Since direct observations of the runoff coefficient is not possible, a distributed hydrological model is required for retrieving this quantity from other sources of observations. Alternatively, one could retrieve soil moisture from satellite data as a surrogate for the runoff coefficient (Wagner et al., 2007, 2008). Thus when interpreting results, it is important to keep in mind that they are conditioned to the underlying model and/or measurement uncertainty. On the other hand, with this analytical framework, outcomes of different models or event characteristics can be more effectively compared and understood.

The framework can be employed for exploring the effects of different types of rainfall events on the generated floods, thus providing hints on the type of monitoring systems required according to the dominant meteorological conditions in flood seasons. Some examples of flood types are presented in Viglione et al. (2010). On the other hand, it can be used to explore the effects of modelling assumptions concerning the actual space–time variability of the simulated variables, thus providing hints for a correct interpretation of the simulated results, for the identification of the actual source of model uncertainty as well as for choosing an effective level of model complexity. For example, from a modelling perspective, the last two covariance terms R3 and R4 in Eq. (9) describe the fraction of the rainfall excess that could be simulated only by employing a distributed model, which explicitly describes the space variability of rainfall and runoff coefficient. A lumped model could compensate for the error due to the spatial averaging by introducing a bias in the simulated average runoff coefficient $W_{x,y}(t)$. The covariance terms, as they potentially assume different values for events with similar spatial averages, are a source of apparent system non-stationarity when the catchment response is simulated with a lumped model.

The framework can be effectively employed for exploring scale effects in catchment flood response (Woods and Sivapalan, 1999). With a change of catchment spatial scale (e.g., from 10 km^2 to 1000 km^2), some relevant factors are reflected in our analytical framework: for example, the importance of channel network travel times generally increases relative to both hillslope travel times, and storm durations; we also expect that the spatial variability terms would become more important because of the proportion of the catchment affected by rainfall (so it will be important where in the catchment does it rain) and because of the variety of geographic settings (big catchments have heterogeneous landscapes and, in many cases, can be divided in a mountainous part upstream and a plain downstream).

The framework can be used to give insight in what are the effects of upscaling and downscaling in modelling (Blöschl and Sivapalan, 1995). Hydrological models represent the catchment storm response by disaggregating (downscaling, interpolating) or aggregating (averaging) field observations, hydrological processes and catchment properties at model (support) scales. Model scales are generally chosen on the basis of the model structure, data availability and simulation objectives. Small model scales imply larger model complexity, thus larger computational effort and larger amounts of data required for model parameterisation and validation (Grayson and Blöschl, 2000). Several field and modelling studies have suggested that only parts of the complete space and time variability appear in the catchment response and that dominant sources of variability can be identified (Seyfried and Wilcox, 1995; Wood, 1995; Blöschl et al., 1995; Woods and Sivapalan, 1999). Other studies showed evidence that the level of model complexity should depend on the dominant processes controlling the catchment response, such as the type of runoff generation mechanism, and the relative timescales of hillslope and network routing (e.g., Nicótina et al., 2008; Atkinson et al., 2002; Jothityangkoon et al., 2001). These studies evaluate the effect of space–time variability by model sensitivity analyses. The results of these studies allow only some general qualitative considerations. More general quantitative conclusions can be draw by employing the framework developed here, since it is not affected by the specific characteristics of the experimental context and the specific model structure.

5. Conclusions

In this paper, we extend the method developed by Woods and Sivapalan (1999) to provide a more general analytical framework for assessing the dependence of the catchment flood response on the space–time interactions between rainfall, runoff generation and routing mechanisms. The analytical framework allows us to quantify explicitly the relative importance of processes and the space–time interactions among them during flood events. Similarly to the St. Venant equations in fluid dynamics, the components of the equations derived here give the order of magnitude with which processes interacts. The additional components added to the original framework of Woods and Sivapalan (1999), i.e., moving storm and hillslope routing variable in space, are demonstrated here to be important and in some cases, in fact, the most important components of flood response.

Acknowledgments

Financial support from the EC (Project No. 037024, HYDRATE) and from the FWF Project P18993-N10 are acknowledged.

Appendix A

A.1. Last term in Eq. (9)

In general, $[\mathrm{cov}_{x,y}(P,W)]_t \neq \mathrm{cov}_{x,y}(P_t,W_t)$ because the covariance is a non-linear operator, which implies that the mean of covariances is not equal to the covariance of the mean. The difference between the two terms is:

$$
\begin{aligned}
&[\mathrm{cov}_{x,y}(P,W)]_t - \mathrm{cov}_{x,y}(P_t,W_t) = \\
&= \frac{1}{T_m}\int_0^{T_m}\left\{\frac{1}{A}\int\int_A [P(x,y,t)-P_{x,y}(t)][W(x,y,t)-W_{x,y}(t)]dx\,dy\right\}dt + \\
&\quad -\frac{1}{A}\int\int_A [P_t(x,y)-P_{x,y,t}][W_t(x,y)-W_{x,y,t}]dx\,dy = \\
&= \frac{1}{A}\int\int_A\left\{\frac{1}{T_m}\int_0^{T_m}[P(x,y,t)-P_{x,y}(t)][W(x,y,t)-W_{x,y}(t)]dt + \right. \\
&\quad \left. -\frac{1}{T_m^2}\left[\int_0^{T_m}[P(x,y,t)-P_{x,y}(t)]dt\right]\left[\int_0^{T_m}[W(x,y,t)-W_{x,y}(t)]dt\right]\right\}dx\,dy = \\
&= \frac{1}{A}\int\int_A\{E([P-P_{x,y}]\cdot[W-W_{x,y}]) - E([P-P_{x,y}])\cdot E([W-W_{x,y}])\}dx\,dy = \\
&= \frac{1}{A}\int\int_A \mathrm{cov}_t([P-P_{x,y}],[W-W_{x,y}])dx\,dy = [\mathrm{cov}_t(P-P_{x,y},W-W_{x,y})]_{x,y}
\end{aligned}
$$

Analogously,

$$[\mathrm{cov}_t(P,W)]_{x,y} - \mathrm{cov}_t(P_{x,y},W_{x,y}) = [\mathrm{cov}_{x,y}(P-P_t,W-W_t)]_t$$

and, consequently,

$$[\mathrm{cov}_t(P-P_{x,y},W-W_{x,y})]_{x,y} = [\mathrm{cov}_{x,y}(P-P_t,W-W_t)]_t$$

This term is also present under the separability assumption in Woods and Sivapalan (1999). If this assumption holds (stationary rainfall and runoff coefficient), then

$$\mathrm{cov}_{x,y}(P,W) = \frac{P_{x,y}(t)}{P_{x,y,t}} \cdot \frac{W_{x,y}(t)}{W_{x,y,t}} \cdot \mathrm{cov}_{x,y}(P_t, W_t)$$

so that

$$[\mathrm{cov}_{x,y}(P,W)]_t - \mathrm{cov}_{x,y}(P_t,W_t) = \frac{\mathrm{cov}_t(P_{x,y},W_{x,y}) \cdot \mathrm{cov}_{x,y}(P_t,W_t)}{P_{x,y,t} \cdot W_{x,y,t}}$$

Note that in example E2 the separability assumption holds and R4 = R2 · R3/R1 (see Table 1). The effect of movement of storm (and runoff coefficient) on the storm-averaged catchment rainfall excess can be written as

$$[\mathrm{cov}_t(P - P_{x,y}, W - W_{x,y})]_{x,y} - \frac{\mathrm{cov}_t(P_{x,y},W_{x,y}) \cdot \mathrm{cov}_{x,y}(P_t,W_t)}{P_{x,y,t} \cdot W_{x,y,t}}$$

analogously to Eqs. (24) and (25).

A.2. From Eq. (11) to Eqs. (13) and (14)

Within a general runoff model, the rainfall excess generated at location (x,y) and at the time-step t is routed to the channel network with a delay $\theta_h(x,y,t)$ [T] and to the outlet with a delay $\theta_n(x,y,t)$ [T]. From Eq. (11) and using the mass conservation property we can write that

$$E(T_q) \cdot \int_0^\infty Q(\tau)d\tau =$$
$$= E(T_q) \cdot \int\int_A \left[\int_0^{T_m} R(x,y,t)dt\right]dx\,dy =$$
$$= \int\int_A \left[\int_0^{T_m} R(x,y,t) \cdot (t + \theta_h(x,y,t) + \theta_n(x,y,t))dt\right]dx\,dy$$

Given the following definitions of the first moment of the temporal distribution of the rainfall excess

$$E(T_r) = \frac{\int\int_A \left[\int_0^{T_m} t \cdot R(x,y,t)dt\right]dx\,dy}{\int\int_A \left[\int_0^{T_m} R(x,y,t)dt\right]dx\,dy} \quad (A.1)$$

the first temporal moment of the hillslope routing distribution

$$E(T_h) = \frac{\int\int_A \left[\int_0^{T_m} R(x,y,t) \cdot \theta_h(x,y,t)dt\right]dx\,dy}{\int\int_A \left[\int_0^{T_m} R(x,y,t)dt\right]dx\,dy} \quad (A.2)$$

and the first temporal moment of the channel routing distribution

$$E(T_n) = \frac{\int\int_A \left[\int_0^{T_m} R(x,y,t) \cdot \theta_n(x,y,t)dt\right]dx\,dy}{\int\int_A \left[\int_0^{T_m} R(x,y,t)dt\right]dx\,dy} \quad (A.3)$$

Eq. (13) follows.

As for the variance

$$\mathrm{Var}(T_q) = E(T_q^2) - [E(T_q)]^2$$

where

$$E(T_q^2) \cdot \int_0^\infty Q(t)dt =$$
$$= \int\int_A \left[\int_0^{T_m} R(x,y,t) \cdot (t + \theta_h(x,y,t) + \theta_n(x,y,t))^2 dt\right]dx\,dy$$

simplifies to

$$E(T_q^2) = E(T_r^2) + E(T_h^2) + E(T_n^2) + 2E(T_rT_h) + 2E(T_rT_n) + 2E(T_hT_n)$$

while

$$[E(T_q)]^2 = [E(T_r)]^2 + [E(T_h)]^2 + [\mathrm{E}(T_n)]^2 + 2E(T_r)E(T_h) + 2E(T_r)E(T_n) + \\ + 2E(T_h)E(T_n)$$

Subtracting $[E(T_q)]^2$ from $E(T_q^2)$ one obtains Eq. (14).

A.3. Towards Eqs. (15), (16) and (18)

For the average time of rainfall excess, given Eq. (A.1), we can write that

$$E(T_r) \cdot \int\int_A \left[\int_0^{T_m} R(x,y,t)dt\right]dx\,dy = A \cdot \int_0^{T_m} t \cdot R_{x,y}(t)dt =$$
$$= AT_m \cdot [T \cdot R_{x,y}]_t$$

so that

$$E(T_r) \cdot AT_m \cdot R_{x,y,t} = AT_m \cdot ([T]_t \cdot [R_{x,y}]_t + \mathrm{cov}_t(T, R_{x,y}))$$

which corresponds to Eq. (15).

For the delay of the hillslope routing, given Eq. (A.2), we can write that

$$E(T_h) \cdot \int\int_A \left[\int_0^{T_m} R(x,y,t)dt\right]dx\,dy =$$
$$= \int\int_A \left[\int_0^{T_m} R(x,y,t) \cdot \theta_h(x,y,t)dt\right]dx\,dy$$

so that

$$E(T_h) \cdot AT_m \cdot R_{x,y,t} = T_m \cdot \int\int_A ([\theta_h]_t \cdot R_t + \mathrm{cov}_t(\theta_h, R))dx\,dy$$

and

$$E(T_h) \cdot AT_m \cdot R_{x,y,t} = AT_m \cdot ([\theta_h]_{x,y,t} \cdot R_{x,y,t} + [\mathrm{cov}_t(\theta_h,R)]_{x,y} + \\ + \mathrm{cov}_{x,y}([\theta_h]_t, R_t))$$

which corresponds to Eq. (16). The same reasoning can be used to derive Eq. (18) from Eq. (A.3).

A.4. Towards Eqs. (20)–(23)

The variance of the time of rainfall excess is

$$\mathrm{Var}(T_r) = E(T_r^2) - [E(T_r)]^2 =$$
$$= E(T^2) + \frac{\mathrm{cov}_t[T^2, R_{x,y}(T)]}{R_{x,y,t}} - [E(T)]^2 - \left[\frac{\mathrm{cov}_t[T, R_{x,y}(T)]}{R_{x,y,t}}\right]^2 +$$
$$- 2E(T) \cdot \frac{\mathrm{cov}_t[T, R_{x,y}(T)]}{R_{x,y,t}} =$$
$$= \mathrm{Var}(T) + \frac{\mathrm{cov}_t[T^2, R_{x,y}(T)]}{R_{x,y,t}} +$$
$$- \frac{\mathrm{cov}_t[T, R_{x,y}(T)]}{R_{x,y,t}} \left[2E(T) + \frac{\mathrm{cov}_t[T, R_{x,y}(T)]}{R_{x,y,t}}\right]$$

which corresponds to Eq. (20) if one considers that T, the time during the rain event, is uniformly distributed between $[0, T_m]$ with distribution $f_T(t) = 1/T_m$ and therefore has variance equal to $T_m^2/12$. The same reasoning can be used to derive Eqs. (21) and (23).

If, as in Woods and Sivapalan (1999), we assume that the hillslope routing can be modeled as a linear reservoir with response time $t_h(x,y)$, since

$$\int_0^\infty \frac{\tau^2}{t_h} \exp\left(-\frac{\tau}{t_h}\right)d\tau = 2t_h^2$$

then

$$\mathrm{Var}(T_h) = E(T_h^2) - [E(T_h)]^2 = \\ = [2t_h^2]_{x,y} + \frac{\mathrm{cov}_{x,y}(2t_h^2, R_t)}{R_{x,y,t}} - [t_h]_{x,y}^2 + -\left[\frac{\mathrm{cov}_{x,y}(t_h, R_t)}{R_{x,y,t}}\right]^2 + \\ - 2[t_h]_{x,y} \cdot \frac{\mathrm{cov}_{x,y}(t_h, R_t)}{R_{x,y,t}}$$

which corresponds to Eq. (22).

A.5. Towards Eqs. (24)–(26)

The covariance between T_r and T_n is

$$\mathrm{Cov}(T_r, T_n) = E(T_r \cdot T_n) - E(T_r) \cdot \ \mathrm{E}(T_n)$$

where

$$E(T_r \cdot T_n) = \frac{\int\int_A \left[\int_0^{T_m} (t \cdot \theta_n) \cdot R(x,y,t)dt\right] dxdy}{\int\int_A \left[\int_0^{T_m} R(x,y,t)dt\right] dxdy} = \\ = \frac{1}{T_m \cdot R_{x,y,t}} \int_0^{T_m} t \cdot \left[\frac{D_{x,y}}{v} \cdot R_{x,y}(t) + \frac{\mathrm{cov}_{x,y}(D,R)}{v}\right] dt = \\ = \frac{1}{v \cdot T_m \cdot R_{x,y,t}} \left\{\int_0^{T_m} t \cdot D_{x,y} R_{x,y} dt + \int_0^{T_m} t \cdot \mathrm{cov}_{x,y}(D,R)dt\right\} = \\ = \frac{1}{v \cdot R_{x,y,t}} \left\{D_{x,y}[T \cdot R_{x,y}]_t + [T \cdot \mathrm{cov}_{x,y}(D,R)]_t\right\} = \\ = \frac{1}{v \cdot R_{x,y,t}} \left\{D_{x,y}\left[\frac{T_m}{2} R_{x,y,t} + \mathrm{cov}_t(T, R_{x,y})\right] + \right. \\ \left. + \frac{T_m}{2}[\mathrm{cov}_{x,y}(D,R)]_t + \mathrm{cov}_t[T, \mathrm{cov}_{x,y}(D,R)]\right\}$$

Subtracting the product of Eqs. (15) and (19), one finds that

$$\mathrm{Cov}(T_r, T_n) = \frac{T_m}{2}\left(\frac{[\mathrm{cov}_{x,y}(D,R)]_t}{v R_{x,y,t}} - \frac{\mathrm{cov}_{x,y}(D,R_t)}{v R_{x,y,t}}\right) + \\ + \frac{\mathrm{cov}_t[T, \mathrm{cov}_{x,y}(D,R)]}{v R_{x,y,t}} - \frac{\mathrm{cov}_t(T, R_{x,y})}{R_{x,y,t}} \cdot \\ \cdot \frac{\mathrm{cov}_{x,y}(D,R_t)}{v R_{x,y,t}} \qquad (A.4)$$

Since D is constant in time, then $[\mathrm{cov}_{x,y}(D,R)]_t = \mathrm{cov}_{x,y}(D,R_t)$ and, since T is constant in space, $[\mathrm{cov}_t(T,R)]_{x,y} = \mathrm{cov}_t(T,R_{x,y})$, obtaining Eq. (25). This simplification would not be possible if v were variable in time. Another formulation for $\mathrm{Cov}(T_r,T_n)$ can be analogously derived in which the term $\mathrm{cov}_t[T,\mathrm{cov}_{x,y}(D,R)]$ is replaced by $\mathrm{cov}_{x,y}[D,\mathrm{cov}_t(D,R)]$.

The covariance between T_r and T_h expressed by Eq. (24) is derived analogously.

As for the last term in Eq. (14), $\mathrm{Cov}(T_h,T_n)$, one proceed as before calculating

$$E(T_h \cdot T_n) = \frac{\int\int_A \left[\int_0^{T_m} (\theta_h \cdot \theta_n) \cdot R(x,y,t)dt\right] dxdy}{\int\int_A \left[\int_0^{T_m} R(x,y,t)dt\right] dxdy} = \\ = \frac{1}{v \cdot R_{x,y,t}} [t_h \cdot D \cdot R_t]_{x,y} = \\ = \frac{1}{v \cdot R_{x,y,t}} \left\{[t_h \cdot D]_{x,y} \cdot R_{x,y,t} + \mathrm{cov}_{x,y}(t_h \cdot D, R_t)\right\} = \\ = \frac{1}{v \cdot R_{x,y,t}} \left\{[t_h]_{x,y} \cdot D_{x,y} \cdot R_{x,y,t} + \mathrm{cov}_{x,y}(t_h, D) \cdot R_{x,y,t} + \mathrm{cov}_{x,y}(t_h \cdot D, R_t)\right\}$$

subtracting the product of Eqs. (17) and (19), and obtaining Eq. (26). Alternative formulations for $\mathrm{Cov}(T_h,T_n)$ are:

$$\mathrm{Cov}(T_h, T_n) = \frac{\mathrm{cov}_{x,y}(t_h, D \cdot R_t)}{v R_{x,y,t}} - \frac{D_{x,y}}{v} \frac{\mathrm{cov}_{x,y}(t_h, R_t)}{R_{x,y,t}} + \\ - \frac{\mathrm{cov}_{x,y}(D, R_t)}{v R_{x,y,t}} \cdot \frac{\mathrm{cov}_{x,y}(t_h, R_t)}{R_{x,y,t}}$$

and

$$\mathrm{Cov}(T_h, T_n) = \frac{\mathrm{cov}_{x,y}(D, t_h \cdot R_t)}{v R_{x,y,t}} - [t_h]_{x,y} \frac{\mathrm{cov}_{x,y}(D, R_t)}{v R_{x,y,t}} + \\ - \frac{\mathrm{cov}_{x,y}(D, R_t)}{v R_{x,y,t}} \cdot \frac{\mathrm{cov}_{x,y}(t_h, R_t)}{R_{x,y,t}}$$

References

Atkinson, S., Woods, R., Sivapalan, M., 2002. Climate and landscape controls on water balance model complexity over changing timescales. Water Resources Research 38 (12), 1314. doi:10.1029/2002WR001487.

Beven, K.J., 1979. Generalized kinematic routing method. Water Resources Research 15 (5), 1238–1242.

Blöschl, G., 2005. On the Fundamentals of Hydrological Sciences. John Wiley & Sons, Chichester. chap. 1.

Blöschl, G., 2006. Hydrologic synthesis: across processes, places, and scales. Water Resources Research 42 (3), W03S02. doi:10.1029/2005WR004319.

Blöschl, G., Sivapalan, M., 1995. Scale issues in hydrological modeling – a review. Hydrological Processes 9 (3–4), 251–290. doi:10.1002/hyp.3360090305.

Blöschl, G., Gutknecht, D., Watzinger, A., 1995. Design Flood for the Erlaufklause Dam, Tech. Rep., Institut für Wasserbau und Ingenieurhydrologie, Technische Universität Wien, Vienna, Austria (in German).

Di Lazzaro, M., 2009. Regional analysis of storm hydrographs in the rescaled width function framework. Journal of Hydrology 373 (3–4), 352–365. doi:10.1016/j.jhydrol.2009.04.027.

D'Odorico, P., Rigon, R., 2003. Hillslope and channel contributions to the hydrologic response. Water Resources Research 39 (5), 1113. doi:10.1029/2002WR001708.

Grayson, R.B., Blöschl, G. (Eds.), 2000. Spatial Patterns in Catchment Hydrology: Observation and Modelling. Cambridge University Press, Cambridge, p. 404.

Jothityangkoon, C., Sivapalan, M., Farmer, D., 2001. Process controls of water balance variability in a large semi-arid catchment: downward approach to hydrological model development. Journal of Hydrology 254 (1–4), 174–198.

Krajewski, W., Georgakakos, K., Jain, S., 1991. A Monte-Carlo study of rainfall sampling effect on a distributed catchment model. Water Resources Research 27 (1), 119–128.

Loague, K., 1988. Impact of rainfall and soil hydraulic property information on runoff predictions at the hillslope scale. Water Resources Research 24 (9), 1501–1510.

McDonnell, J.J., Woods, R., 2004. On the need for catchment classification. Journal of Hydrology 299 (1–2), 2–3. doi:10.1016/j.jhydrol.2004.09.003. editorial.

Michaud, J., Sorooshian, S., 1994. Comparison of simple versus complex distributed runoff models on a midsized semiarid watershed. Water Resources Research 30 (3), 593–605.

Naden, P.S., 1992. Spatial variability in flood estimation for large catchments – the exploitation of channel network structure. Hydrological Sciences – Journal – des Sciences Hydrologiques 37 (1), 53–71.

Nicótina, L., Alessi Celegon, E., Rinaldo, A., Marani, M., 2008. On the impact of rainfall patterns on the hydrologic response. Water Resources Research 44 (12), W12401. doi:10.1029/2007WR006654.

Obled, C., Wendling, J., Beven, K.J., 1994. The sensitivity of hydrological models to spatial rainfall patterns – an evaluation using observed data. Journal of Hydrology 159 (1–4), 305–333.

Ogden, F.L., Julien, P.Y., 1994. Runoff model sensitivity to radar rainfall resolution. Journal of Hydrology 158 (1–2), 1–18.

Ogden, F.L., Richardson, J.R., Julien, P.Y., 1995. Similarity in catchment response. 2. Moving rainstorms. Water Resources Research 31 (6), 1543–1547.

Pilgrim, D.H., 1976. Travel times and nonlinearity of flood runoff from tracer measurements on a small watershed. Water Resources Research 12 (3), 487–496.

Rinaldo, A., Marani, A., Rigon, R., 1991. Geomorphological dispersion. Water Resources Research 27 (4), 513–525.

Robinson, J., Sivapalan, M., Snell, J., 1995. On the relative roles of hillslope processes, channel routing, and network geomorphology in the hydrologic response of natural catchments. Water Resources Research 31 (12), 3089–3101.

Rodriguez-Iturbe, I., Valdes, J., 1979. Geomorphologic structure of hydrologic response. Water Resources Research 15 (6), 1409–1420.

Saco, P., Kumar, P., 2002. Kinematic dispersion in stream networks – 1. Coupling hydraulic and network geometry. Water Resources Research 38 (11), 1244. doi:10.1029/2001WR000695.

Sangati, M., Borga, M., Rabuffetti, D., Bechini, R., 2009. Influence of rainfall and soil properties spatial aggregation on extreme flash flood response modelling: an evaluation based on the Sesia river basin, North Western Italy. Advances in Water Resources 32 (7), 1090–1106. doi:10.1016/j.advwatres.2008.12.007.

Seyfried, M., Wilcox, B., 1995. Scale and the nature of spatial variability – field examples having implications for hydrologic modeling. Water Resources Research 31 (1), 173–184.

Shah, S., O'Connell, P., Hosking, J., 1996a. Modelling the effects of spatial variability in rainfall on catchment response. 1. Formulation and calibration of a stochastic rainfall field model. Journal of Hydrology 175 (1–4), 67–88.

Shah, S., O'Connell, P., Hosking, J., 1996b. Modelling the effects of spatial variability in rainfall on catchment response. 2. Experiments with distributed and lumped models. Journal of Hydrology 175 (1–4), 89–111.

Sivapalan, M., 2005. Pattern, Process and Function: Elements of a Unified Theory of Hydrology at the Catchment Scale. Encyclopedia of Hydrological Sciences. John Wiley & Sons, Chichester (Chapter 13).

Skøien, J.O., Blöschl, G., 2006. Catchments as space–time filters – a joint spatio-temporal geostatistical analysis of runoff and precipitation. Hydrology and Earth System Sciences 10 (5), 645–662.

Skøien, J.O., Blöschl, G., Western, A., 2003. Characteristic space scales and timescales in hydrology. Water Resources Research 39 (10), 1304. doi:10.1029/2002WR001736.

Viglione, A., Chirico, G.B., Komma, J., Woods, R., Borga, M., Blöschl, G., 2010. Quantifying space–time dynamics of flood event types. Journal of Hydrology 394 (1–2), 213–229. doi:10.1016/j.hydrol.2010.05.041.

Wagener, T., Sivapalan, M., Troch, P., Woods, R., 2007. Catchment classification and hydrologic similarity. Geography Compass 1 (4), 901–931. doi:10.1111/j.1749-8198.2007.00039.x.

Wagner, W., Blöschl, G., Pampaloni, P., Calvet, J.-C., Bizzarri, B., Wigneron, J.-P., Kerr, Y., 2007. Operational readiness of microwave remote sensing of soil moisture for hydrologic applications. Nordic Hydrology 38 (1), 1–20.

Wagner, W. et al., 2008. Temporal stability of soil moisture and radar backscatter observed by the advanced synthetic aperture radar (asar). Sensors 8 (2), 1174–1197.

Western, A., Blöschl, G., Grayson, R.B., 2001. Toward capturing hydrologically significant connectivity in spatial patterns. Water Resources Research 37 (1), 83–97.

Winchell, M., Gupta, H., Sorooshian, S., 1998. On the simulation of infiltration- and saturation-excess runoff using radar-based rainfall estimates: Effects of algorithm uncertainty and pixel aggregation. Water Resources Research 34 (10), 2655–2670.

Wood, E.F., 1995. Scaling behavior of hydrological fluxes and variables – empirical-studies using a hydrological model and remote-sensing data. Hydrological Processes 9 (3–4), 331–346.

Woods, R., 1997. A search for fundamental scales in runoff generation: combined field and modelling approach. Ph.D. Thesis, Department of Environmental Engineering, University of Western Australia, Nedlans, Western Australia.

Woods, R., Sivapalan, M., 1999. A synthesis of space–time variability in storm response: rainfall, runoff generation, and routing. Water Resources Research 35 (8), 2469–2485.